On the Linearity of Turbomachinery Interaction Noise. Part I: 2D Analysis

Journal:	*17th AIAA/CEAS Aeroacoustics Conference (32nd AIAA Aeroacoustics Conference)*
Manuscript ID:	1017944
luMeetingID:	2483
Date Submitted by the Author:	31-May-2011
Contact Author:	Fernandez Aparicio, Jose Ramon

On the Linearity of Turbomachinery Interaction Noise. Part I: 2D Analysis

José Ramón Fernández Aparicio*, **Adolfo Serrano**† **and Raúl Vázquez**‡
ITP, Industria de Turbo Propulsores, San Fernando de Henares, Madrid, 28830, Spain

Abstract

This paper is intented to analyze the linearity of turbomachinery tone noise interaction with application to Low Pressure Turbines (LPTs). This is investigated by the comparison of non-linear and linearized CFD models in different test cases. To begin with, a methodology for predicting interaction noise based on independent and single rows calculations is presented. The method is applied to a couple of 2D models; one corresponds to an inviscid fan where the problem is supposed to be linear. The other is a 2D viscous model of a LPT where the linearity can depend on the gap between rows. The extension to 3D models, including a 'state of the art' LPT stage, is planned to be published as a second part in 2012. Non-linear and linear simulations are performed using Mu^2s^2T Suite, that is an in-house RANS CFD set of tools, with proven capability for performing aeroacoustic simulations [5, 8]. Non-linear simulations are calculated in time domain, using dual time step and phased lagged boundary conditions at the periodic domains. Non-linear and linearized solutions use the same grid, numerical scheme, turbulent model and unsteady boundary conditions at inlet/outlet domains. Temporal harmonics from the non-linear simulations are computed for each row and compared with those estimated from the linear model. Results are mainly based on the acoustic field up and downstream the interacting machine.

Nomenclature

$[A]$	Transference matrix in LMSOL
$[A]_{kl}$	Single influence matrix of mode k and scattered mode l, included in [A]
$[U]$	Perturbation vector in LMSOL
$[U]_k$	Single spinning mode k perturbation vector, included in [U]
γ	Ratio of specific heats
Ω	Rotational Shaft Speed
ω	Non-steady frequency
$\overrightarrow{x}$	Vector position in cartesian coordinates
ρ	Density
$\tilde{\tilde{()}}$	Time averaged flow variable
$\widetilde{()}$	Ensemble averaged flow variable
B	Number of rotor blades
BPF	Blade Passing Frequency
c_0	Ambient speed of sound
C_R	Rotor chord
C_S	Stator chord
CFD	Computational Fluid Dynamics

*Aeroacoustics Engineer, Aerodynamic Technology Dept. ITP. E-mail: joseramon.fernandez@itp.es
†Senior Engineer on Aeroacoustics, Aerodynamic Technology Dept. ITP. E-mail: adolfo.serrano@itp.es
‡Head of Aerodynamic Technology Dept. ITP, Associate Professor, School of Aeronautics, UPM. E-mail: raul.vazquez@itp.es

g/c	Gap to chord ratio
i	Iteration Index
j	Gap Index
k_x	Axial Wave Number
k_y	Transverse Wave Number
LEE	Linearized Euler Equations
$LMSOL$	Linear Method Solver
LNS	Linearized Navier Stokes
LPT	Low Pressure Turbine
$LRANS$	Linearized Reynolds Averaged Navier Stokes
LST	Lifting Surface Theory
M	Number of ensemble averages in Ensemble Averaged Operator
m	Ensemble average Index
M_r	Relative Mach Number
M_x	Axial Mach Number
MPI	Message Passing Interface
p	Pressure
$p_i^{+,j}$	Downstream propagating pressure at iteration i and gap j
$p_i^{-,j}$	Upstream propagating pressure at iteration i and gap j
$RANS$	Reynolds Averaged Navier Stokes
T	Turbomachine Period for Time Averaged Filter
t	Temporal coordinate
u	Axial velocity
$u_i^{v,j}$	Convected Vorticity at iteration i and gap j
$UNRBC$	Unsteady Non-Reflecting Boundary Conditions
$URANS$	Unsteady Reynolds Averaged Navier Stokes
V	Number of stator vanes
v	Transversal velocity
x	Axial coordinate
y	Transverse coordinate
y^+	Dimensionless wall distance
$()'$	Deterministic flow variable in frequency domain
$()^d$	Deterministic flow variable
$()^e$	Non-deterministic flow variable
$()_0$	Steady flow variable

I. Introduction

Turbine noise is a significant contributor to the overall aircraft noise signature. Continuing efforts to effectively decrease other typically dominant sources of noise (fan and jet), together with requirements to have more efficient and lighter turbines, might have as a result that past practices to make cut-off turbines will not be sufficiently quiet. Hence, very high effort has been put in turbine noise research with important achievements on the understanding of the dominant generation mechanisms that allow distinguishing quiet from loud turbines [4, 12, 18, 19]. However, the state of the art highlights that there exist applications in which turbine noise is not fully understood being a source of mis-prediction [16, 25].

The convenience of CFD techniques for achieving further turbine tone noise reductions have been raised in the past [10, 11, 12, 24]. However, it seems there is not agreement on the most suitable CFD model for those purposes. Kennepohl [12] uses Linearized Euler Equations (LEE) for the computation of turbine tone noise and, although absolute levels differ from the experiments, tendencies seem to be well captured. Escribano [11] compares Linearized Navier Stokes (LNS) and LEE for turbine 2D profiles concluding that viscous effects are of first order and should be retained in the computation of turbine noise. More recently, Broszat [4] and Pinelly [17] obtain results closer to experiments when using LEE with a viscous base or steady flow, and Van-Zante [24] addresses the same problem

using non-linear CFD (URANS) assuming the flow is sufficiently complex to be linearized. Controversy is also present in fan tone noise prediction, although this phenomenon here has been much more investigated. Linearity of the fan interaction tone is early demonstrated by Sijtsma [21] for a simple test case using the Lifting Surface Theory (LST) developed by Schulten [22]. Envia [9] uses LEE over Euler based flows for fan rigs and generally obtains better agreement than the same model used in turbines [12]. Sharma [20] concludes that the inclusion of RANS steady solutions with LEE does not necessarily conduce to more accurate results, and Maunus [15] analyzes the high influence of the rotor wake profiles in the emitted acoustic power.

The most suitable CFD model (LEE, LNS, RANS or Euler base flow, URANS) will be highly dependent on the particular case, and a general conclusion is difficult to be extracted being subject of further discussions in the future. Under these circumstances, the intention of this paper is to give more insight on how significant can be the non-linear effects in the interaction noise, firstly analyzing 2D models that allow more flexibility and clarity on some of the effects to be pursued, secondly extending this methodology to 3D geometries, something that will be addressed in a second part of this paper to be published in 2012.

In those cases in which URANS and LRANS models are expected to conduce to similar results, i.e., interaction noise can be linearized, the selection of the most suitable one can be dependent on several factors. One of these is the computational cost, which is generally higher for the URANS methods. However, in some applications the number of necessary linear calculations can make LRANS models be more time-consuming than the 'all in one run' URANS. Another clear advantage that LRANS models offer is the capability of splitting the unsteady field, so that the contribution of the different unsteady effects to the overall noise can be assessed.

As mentioned, 2D simulations are specially interesting since the linearity related to the profile aerodynamics can be analyzed independently, so that dependencies like gap to chord distance can be isolated from 3D effects. Besides, the non-reflecting boundary conditions imposed at inlet and outlet are expected to work better than in the 3D case, so that uncertainties due to spurious reflections near the boundaries might be small. Since the grid size is considerably lower, 2D simulations are low time-consuming and make them have great flexibility, consequently, several simulations have been done for assessing the dependence on the distance between interacting rows. The first test case is an inviscid fan without loading, since the perturbations are much lower than the base flow and the interaction will be linear even for small distances between the rows. Therefore, this first case can be considered as a verification of the linear methodology and can give a first assessment of the uncertainties when modeling based on single row calculations. The second test case is a viscous LP turbine profile where the dependence with the distance is also analyzed as it is expected to play an important role in concluding with regard linearity.

II. Fundamentals of Unsteady and Linearized Reynolds Averaged Flow Models

The purpose of this section is to highlight the fundamentals of the two models analyzed in this paper, URANS and LRANS, and identify which terms are retained and the assumptions that are made. A more detailed description of the models can be found in Mu^2s^2T related references [5, 7, 8]. The common basis they have is the resolution of the Reynolds Averaged Navier Stokes (RANS) equations. That implies the deletion of the non-deterministic unsteady structures associated to the turbulent flow by means of filtered solutions. The extension of this model to obtain the unsteady solutions of deterministic structures conduces to the URANS models that can be simplified to LRANS under certain circumstances.

II.A Ensemble and Time Averaged Filters

URANS and LRANS models are described by the introduction of the ensemble and time averaged operators, following the definition proposed by Adamczyk [1, 2]. It is assumed that the unsteady flow can be decomposed in three components, i.e., one averaged 'steady' solution that is not time dependent, and two unsteady disturbances. These are a non-deterministic component associated to turbulence intensities and another deterministic associated to relative movements between rotatory and stationary parts of the turbomachinery, which are harmonic oscillations related to the shaft speed of the device. In other words, if u is a flow variable, i.e. axial velocity, it can be decomposed as:

$$u\left(\overrightarrow{x},t\right)=u_0\left(\overrightarrow{x}\right)+u^e\left(\overrightarrow{x},t\right)+u^d\left(\overrightarrow{x},t\right) \tag{1}$$

Non-deterministic disturbances can be filtered out from the Navier-Stokes equations by the introduction of the ensemble averaged operator. In a mathematical form, it is defined as:

$$\widetilde{u}\left(\overrightarrow{x},t\right)=\lim_{M\to\infty}\frac{1}{M}\sum_{m=1}^{M}u\left(\overrightarrow{x},t+\frac{2\pi}{\Omega}\left(m-1\right)\right)=u_0\left(\overrightarrow{x}\right)+u^d\left(\overrightarrow{x},t\right) \tag{2}$$

Being M the number of ensemble averages based on turbomachine periods and Ω the shaft speed. In other words, when evaluating the unsteady variable at the same position relative to one period during a sufficient number of them, the non-deterministic disturbances can be filtered out, in a way that $\widetilde{u}_0\left(\overrightarrow{x}\right)=u_0\left(\overrightarrow{x}\right),\widetilde{u}^d\left(\overrightarrow{x},t\right)=u^d\left(\overrightarrow{x},t\right),\widetilde{u}^e\left(\overrightarrow{x},t\right)=0$. The inclusion of these filters on the Navier-Stokes equations conduces to the Reynolds Averaged form in which the non-deterministic fluctuations are retained in the so-called Reynolds Stresses in the Momentum and Energy equations. The accomplishment of the $u_0\left(\overrightarrow{x}\right)+u^d\left(\overrightarrow{x},t\right)$ field implies the resolution of the Unsteady Reynolds Averaged Navier Stokes equations (URANS), having in mind that the unsteadiness that is being pursued comes from deterministic disturbances due to the presence of relative motion between rows. Going one step further, URANS model can be simplified to a LRANS model assuming that $u^d\left(\overrightarrow{x},t\right)\lll u_0\left(\overrightarrow{x}\right)$. For simplification, assuming u is the axial velocity and evaluating the incompressible convective term in the axial direction:

$$\widetilde{u}\left(\overrightarrow{x},t\right)\frac{\partial\widetilde{u}\left(\overrightarrow{x},t\right)}{\partial x}=u_0\left(\overrightarrow{x}\right)\frac{\partial u_0\left(\overrightarrow{x}\right)}{\partial x}+u^d\left(\overrightarrow{x},t\right)\frac{\partial u_0\left(\overrightarrow{x}\right)}{\partial x}+u_0\left(\overrightarrow{x}\right)\frac{\partial u^d\left(\overrightarrow{x},t\right)}{\partial x}+u^d\left(\overrightarrow{x},t\right)\frac{\partial u^d\left(\overrightarrow{x},t\right)}{\partial x} \tag{3}$$

The first term on the right hand of Eq.3 corresponds to the assumption that deterministic unsteadiness is small enough and have no influence on the main flow, in other words, a RANS 'single row' steady solution. The second and third terms assume the unsteady (deterministic) disturbances do not influence the main or base flow and therefore they can be modeled as small perturbations, constituting the hypothesis of the LRANS models. The fourth term accounts the non-linearity of the unsteady flow, having an influence on the unsteady field $u^d\left(\overrightarrow{x},t\right)$ but also on the main flow $u_0\left(\overrightarrow{x}\right)$. Adamczyk [2] goes one step further and introduces the time averaged filter as:

$$\tilde{\widetilde{u}}\left(\overrightarrow{x},t\right)=\frac{1}{T}\int_0^T\widetilde{u}\left(\overrightarrow{x},t\right)dt=u_0\left(\overrightarrow{x}\right) \tag{4}$$

, being T the period of the turbomachine. When introducing the ensemble and time averaged filters on the Navier Stokes equations, they conduce to the deterministic form of the Navier Stokes equations in which, besides the Reynolds stresses due to the presence of non-deterministic fluctuations, another set of stresses related to the fourth term on the right hand of Eq.3 will affect the main or base flow $u_0\left(\overrightarrow{x}\right)$. Time averaged solutions and the characterization of the deterministic stresses are out of the scope of this paper, so that steady solutions of the LRANS models will be obtained by 'single-row' RANS calculations. Discrepancies between time averaged URANS flow and RANS will also be subject of analysis and comparison for the LP Turbine profile test case in Section 5. The validity of the linear assumptions will depend on the importance of the last term in Eq.3, as well as on the assumption of small perturbations that allows the uncoupling of the steady and the unsteady field.

II.B Codes Description

Both URANS and LRANS solutions will be obtained with Mu^2s^2T suite, that is a in-house solver with hybrid unstructured grids to discretize the spatial domain and an edge-based data structure to compute the fluxes. A second-order numerical scheme conforms the spatial discretization scheme. A time-marching technique has been implemented with an explicit five-stage Runge-Kutta. Multigrid techniques [7] are used to accelerate steady state convergence. The code is able to run parallelized using MPI.

When URANS calculations are considered, Navier-Stokes equations must be integrated forward in time. Mu^2s^2T uses a second order dual-time step scheme for unsteady computations, and phased-lagged boundary conditions at

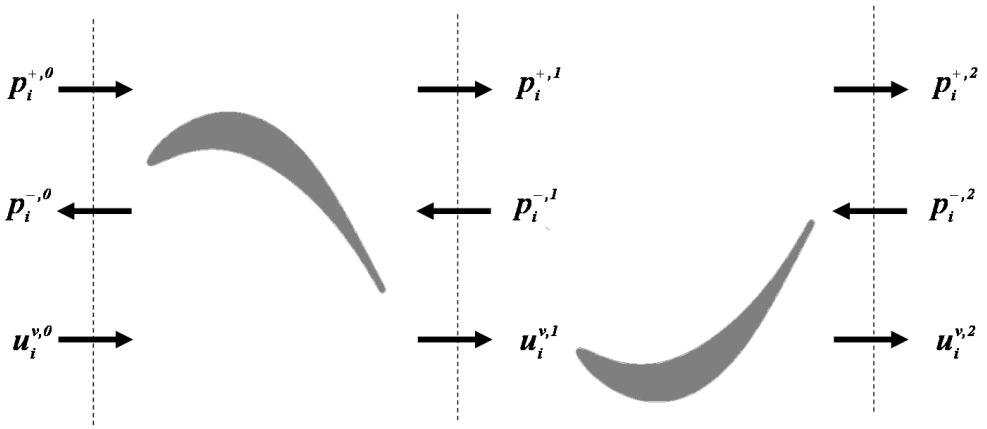

Figure 1: Waves existing in a case with two rows and one mode investigated

periodic domains [6]. The capability of Mu^2s^2T to cope with unsteady simulations in turbomachines has been already demonstrated [5].

Linear version of Mu^2s^2T, that is Mu^2s^2T-L, solves the viscous linearized Navier-Stokes equations in conservative form. The spatial discretization is obtained linearizing the discretized equations of the non-linear version of the code. A steady solution is required and the steady non-linear solution is usually used. The grids used for the non-linear and the linearized solvers are identical and hence the spatial discretization of the latter is fully consistent with that of the former. The spatial domain is therefore discretized using hybrid unstructured grids with edge-based data structure. The code is marched in pseudo-time using a Runge-Kutta scheme. Convergence is also accelerated using a multigrid scheme. Unsteady, 2D, exact non-reflecting boundary conditions [13] are imposed at inlet / outlet calculation domains at each radius. As in the non-linear version, the capability of Mu^2s^2T-L to perform unsteady simulations in turbomachines has been already demonstrated [8].

III. Linear Methodology Description

The objective of this section is defining a methodology for the construction of a multirow and multimode unsteady field based on the sum of independent and one row calculations. Consequently, it is pursued the same objective than Heinig [14] but, instead of using an electrical analogy, the unsteady field can be constructed with an hypothetical temporal process. Starting from the noise generation mechanisms (wakes and potential fields), different interaction sources are being generated and transmitted at each iteration. Mathematically, the method is more complex; however, it can be generalized to more general flows and it can also include scattering effects. The methodology is implemented in a code called LMSOL.

To start with, let's considered a 2D flow and only two rows with the presence of only one spinning mode of interest. Steady or base flow is assumed to be sufficiently uniform so that the wave-splitting methodology included in the Appendix can be used to decompose the unsteady field in up/downstream acoustic propagating and vorticity waves. Entropy disturbances will be ignored in this study. Figure 1 shows the nomenclature that will be followed for the acoustic disturbances at a given virtual iteration i located in the gap j: $p_i^{+,j}$ is the downstream acoustic propagating, $p_i^{-,j}$ stands for the upstream acoustic and $u_i^{v,,j}$ for the convected vorticity.

The magnitudes of the iteration $i+1$ will be the result of the iteration i sources interacting with any of the two rows. Three different mechanisms are identified, schematically shown in Figure 2: downstream/upstream acoustic transmission and vorticity interaction. This is expressed as:

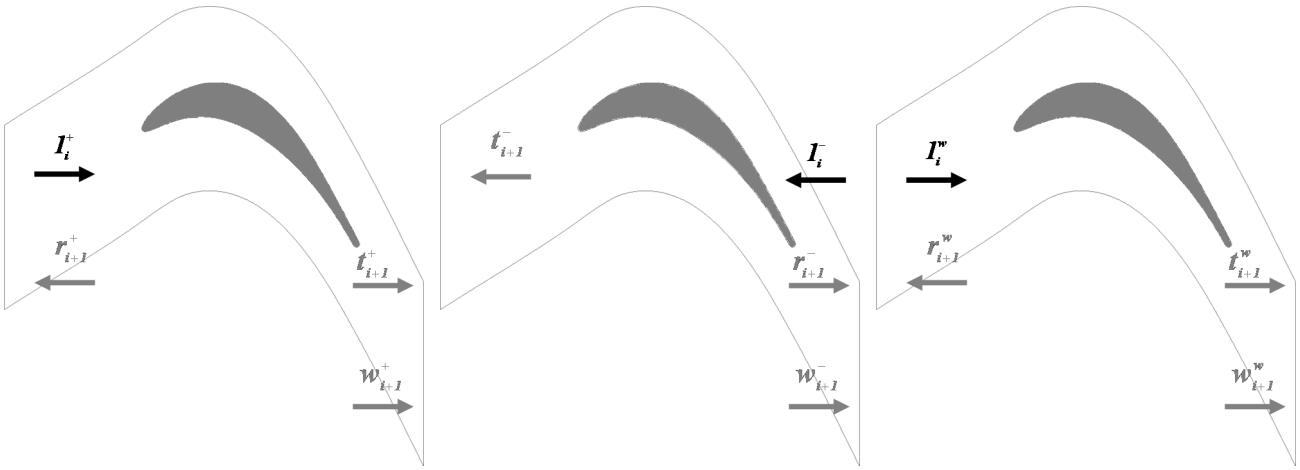

Figure 2: Possible interactions in a generic row: downstream transmission (left), upstream transmission (middle) and vorticity interaction (right)

$$\begin{bmatrix} p^{+,0} \\ p^{-,0} \\ u^{v,0} \\ p^{+,1} \\ p^{-,1} \\ u^{v,1} \\ p^{+,2} \\ p^{-,2} \\ u^{v,2} \end{bmatrix}^{i+1} = \begin{bmatrix} 0 & 0 & 0 & 0 & 0 & 0 & 0 & 0 & 0 \\ r_{0-1}^{+} & 0 & r_{0-1}^{v} & 0 & t_{0-1}^{-} & 0 & 0 & 0 & 0 \\ 0 & 0 & 0 & 0 & 0 & 0 & 0 & 0 & 0 \\ t_{0-1}^{+} & 0 & t_{0-1}^{v} & 0 & r_{0-1}^{-} & 0 & 0 & 0 & 0 \\ 0 & 0 & 0 & r_{1-2}^{+} & 0 & r_{1-2}^{v} & 0 & t_{1,2}^{-} & 0 \\ w_{0-1}^{+} & 0 & w_{0-1}^{v} & 0 & w_{0-1}^{-} & 0 & 0 & 0 & 0 \\ 0 & 0 & 0 & t_{1-2}^{+} & 0 & t_{1-2}^{v} & 0 & r_{1,2}^{-} & 0 \\ 0 & 0 & 0 & 0 & 0 & 0 & 0 & 0 & 0 \\ 0 & 0 & 0 & w_{1-2}^{+} & 0 & w_{1-2}^{v} & 0 & w_{1,2}^{-} & 0 \end{bmatrix} \cdot \begin{bmatrix} p^{+,0} \\ p^{-,0} \\ u^{v,0} \\ p^{+,1} \\ p^{-,1} \\ u^{v,1} \\ p^{+,2} \\ p^{-,2} \\ u^{v,2} \end{bmatrix}^{i} \tag{5}$$

The first term on the right hand is the transfer matrix $[A]$, which relates the perturbations vector $[U]$ at an iteration $i+1$ with the same vector at the iteration i.

$$[U]^{i+1} = [A] \cdot [U]^{i} \tag{6}$$

Matrix $[A]$ will be filled with 18 coefficients, being the number of independent linear calculations $18/3 = 6$, 3 for each of the 2 rows. The iterative process starts with a set of initial sources (generation) located at each gap and iterating until the amplitude of the perturbations vector at the iteration n is sufficiently small. The total amplitude is then calculated with the sum of the perturbations obtained at every iteration:

$$[U] = \sum_{i=1}^{n} [U]^{i} \tag{7}$$

The extension to more spinning modes included can be easy with this formulation. For instance, if three modes are considered, the perturbation vector $[U]$ can be decomposed into single spinning mode vectors $[U]_1$,$[U]_2$,$[U]_3$, and the transfer matrix $[A]$ in single influence matrices $[A]_{kl}$, being k the incoming mode and l the resulted scattered mode. Mathematically can be expressed as:

$$\begin{bmatrix} U_1 \\ U_2 \\ U_3 \end{bmatrix}^{i+1} = \begin{bmatrix} A_{11} & A_{12} & A_{13} \\ A_{21} & A_{22} & A_{23} \\ A_{31} & A_{32} & A_{33} \end{bmatrix} \cdot \begin{bmatrix} U_1 \\ U_2 \\ U_3 \end{bmatrix}^{i} \tag{8}$$

The number of necessary coefficients will be 18x9 = 162 and the number of required simulations will be 162/9 = 18 that is 9 for each of the 2 rows.

BUILD	Gap/chord
1	0.1064
2	0.2504
3	0.3752
4	0.6560
5	0.9368

Table 1: Non-linear simulations performed for the low-speed fan case: each build correspond to a different value of the gap distance between the rows.

Similarly, the method can be applied to more rows and also 3D flows considering both spinning and radial modes. As expected, the limitation of this method will be the number of required single row calculations, i.e., for a modern 6 stage LP turbine, the minimum number with no scatter or reflections will be more than 300 [10]. Under these circumstances, the identification of the dominant mechanisms is essential to be able to predict multistage noise levels with a reasonable number of single row calculations.

IV. Application to an Inviscid Fan with No Loading

The first geometry investigated is a 2D rotor-stator configuration inspired from the mid-section of the low-speed fan that Sijtsma [21] used for the validation of the Lifting Surface Theory (LST). The rotor consists of 16 blades of 40 mm. chord length, with a modified NACA 010-35 section which stagger angle has been adjusted to have no incidence at the shaft speed simulated of 5550 rpm. The stator is formed of 16 vanes aligned with an axial uniform flow. The streamwise section is uncambered NACA 010-135 wing section with a 10% thickness and 50 mm. chord length. The number of vanes have been modified from the 18 that originally had [21] to 16 in order to avoid the use of phase-lagged conditions and save computational cost. 2D simulation that is performed corresponds to 50% span height, that is a constant radius of 160 mm.

Figure 3 shows a schematic view of the geometries together with a representation of the five gap distances used in the URANS simulations performed with Mu^2s^2T. The distance between the rows is modified between a 10% and 94% of the rotor chord (Table 1) in order to evaluate the conditions when the non-linear effects could become important. The 'original' gap distance corresponds to build 3. Only one pitch has been simulated with imposition of periodicity at any time since the number of vanes and blades coincide. The grid used is unstructured, with a grid criteria based on at least 40 points per wavelength desired and a minimum number of points in the blade to properly solve the steady aerodynamics [11]. The resulting number of nodes goes from 130000 to 170000 depending on the gap distance between the rows. Inlet and outlet gaps are about a 150% of axial chord, seen long enough to avoid reflections as 1D Unsteady Non-Reflecting Boundary Conditions (UNRBC) have been imposed. The communication between the two rows has been done through the slide plane [5, 6].

Figure 4-left shows the amplitudes of the three spinning modes of interest for the first Blade Passing Frequency (BPF), i.e., Mode 16 that corresponds to the Blade perturbation, Mode -16 for the Vane and Mode 0 that is the Tyler&Sofrin mode [23] resulting of the interaction between rows. The potential field of each row interacting with the other is the only mechanism responsible of the generation of interaction Mode 0, and their amplitude depend linearly with the axial distance (in dB). The slopes are $\pm\frac{B\sqrt{1-M_r^2}}{1-M_x^2}$for the Blade and $\pm\frac{V}{\sqrt{1-M_x^2}}$ for the Vane, being M_x and M_r the axial and relative Mach Number respectively. Potential sources at leading and trailing edge are 152 dB for the rotor and about 141 dB for the stator. Having in mind that the base static pressure is 100000 Pa, that implies the maximum disturbance is 0.8% for the rotor and 0.2% the stator. In other words, cross terms appearing in the fourth term on the right hand of Eq.3 will be about 1000 times lower than the linear term, so that the unsteady flow can be linearized even when the gap between the rows is small. Figure 5 shows the spinning modes appearing in Figure 4-left but split into up and downstream propagating / decaying waves, assuming they are being propagated in an uniform flow and following the formulation shown in the Appendix. From the observation of the figure, it can be seen that there are no reflections at the boundaries except some spurious levels for the cut-off modes +16 and -16 that have not an influence on the interaction process since the inlet and outlet gaps are sufficiently large.

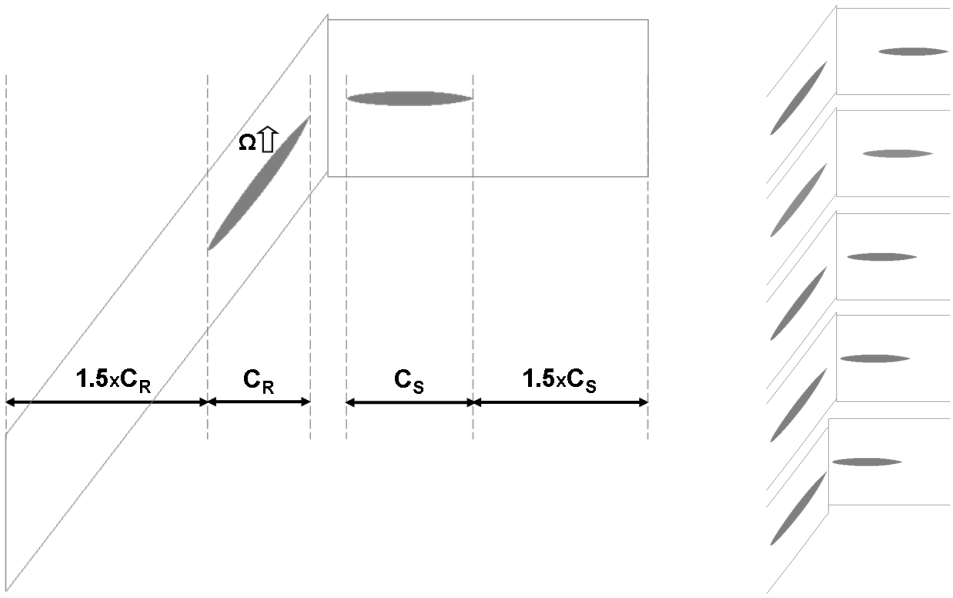

Figure 3: Schematic view of the 2D simulation of the low-speed fan case. Build 3 is represented in the left plot. Right figure represents the five builds with the gap investigated.

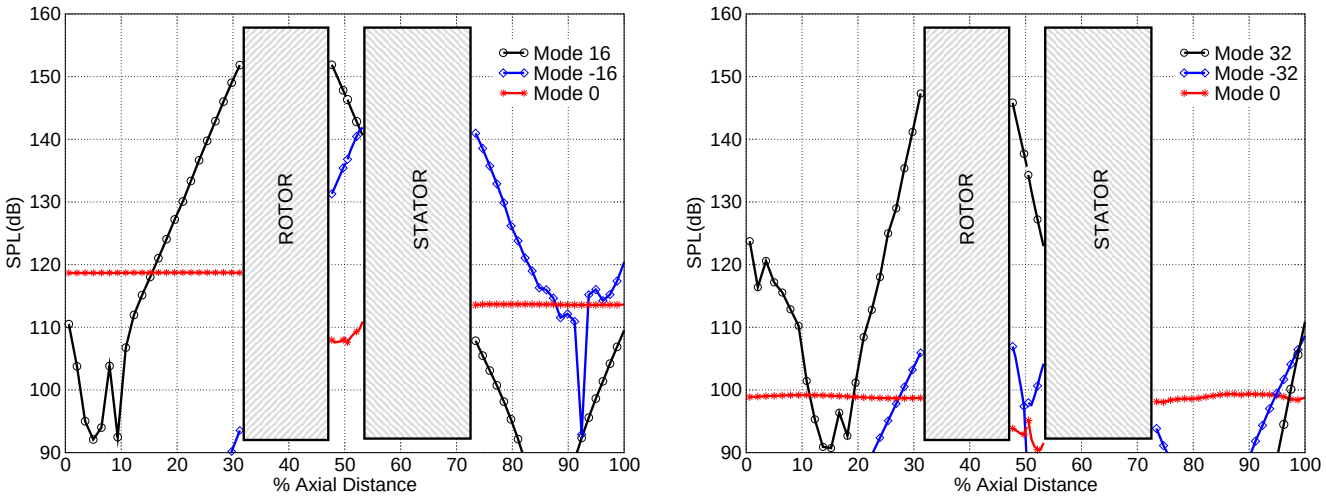

Figure 4: Inviscid Fan with No Loading Build 3 URANS solution: Spinning mode amplitudes of the relevant modes contributing to the 1BPF (left) and 2BPF (right) interaction noise.

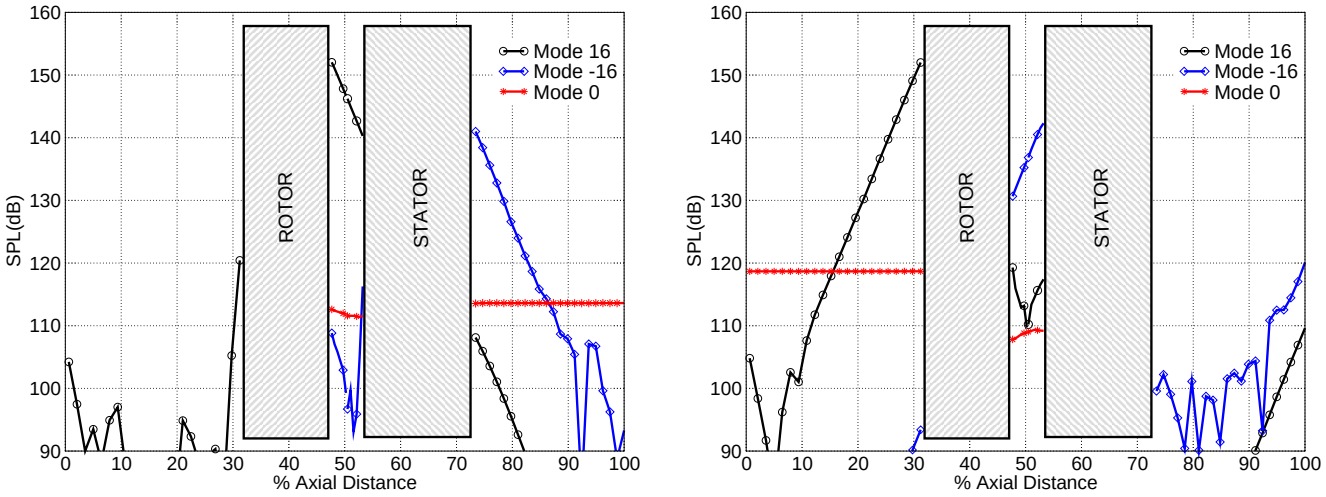

Figure 5: Inviscid Fan with No Loading Build 3 URANS solution: Spinning mode amplitudes of the relevant modes contributing to the 1BPF. Downstream Propagating / Decaying waves (left). Upstream Propagating / Decaying waves (right).

In order to use the linear methodology presented in Section 3, it is first necessary to decide the number of spinning modes to take into account. Given that the number of linear calculations will grow with the number of modes considered, it is important to consider as low number as possible. On the one hand, mode 0 is included as the interaction noise is the objective of the investigation. On the other hand, and according to the results obtained with the URANS simulation for build 3 (g/c = 0.3752) shown in Figure 4-left, the potential field coming from blade and vane are of the same order of importance and would need to be considered in the analysis. Figure 4-right shows the same results for the second harmonics. Since they are about 10 dB lower than first harmonics and would need to disturb them through a scattering phenomena, a low importance of their contribution is expected. Thus the modes included in the analysis are those corresponding to 16, -16 and 0.

The number of linear calculations also grows with the number of single row interactions considered at each mode. Although LMSOL requires three interaction mechanisms at each mode and row (downstream propagating pressure, upstream propagating pressure and vorticity), only LRANS simulations of the mechanisms assumed to be dominant have been run. These are the following:

- Potential field of stator upstream propagating and interacting with the rotor (mode -16,-)
- Potential field of rotor upstream propagating and interacting with the rotor (mode 16,+)
- Transmission through the rotor of interaction mode propagating upstream (mode 0,-)
- Transmission through the stator of interaction mode propagating downstream (mode 0,+)

The information obtained with these simulations, as well as that extracted from the non-linear case, is managed for the use of LMSOL. To summarize:

- The interaction noise is assumed to be dominated by four independent mechanisms that are linear simulated. Two are associated to generation and other two are associated to the transmission process. These four simulations are used to compute the transmission and reflection coefficients of the main perturbations that exist in the problem, being the rest set to 0.
- The single row domains in which the linear simulations are performed do not necessarily need to be the same as in the non-linear domain. This is specially interesting in the short gaps build, but also that the gap to chord dependence can be reconstructed with only one set of linear simulations. That will also apply to the initial generation sources. The gaps used for the single row linear simulations needs to have inlet and outlet gaps long enough to allow the boundary condition to work, but short enough not to have the waves with such low amplitude that they are not properly solved.

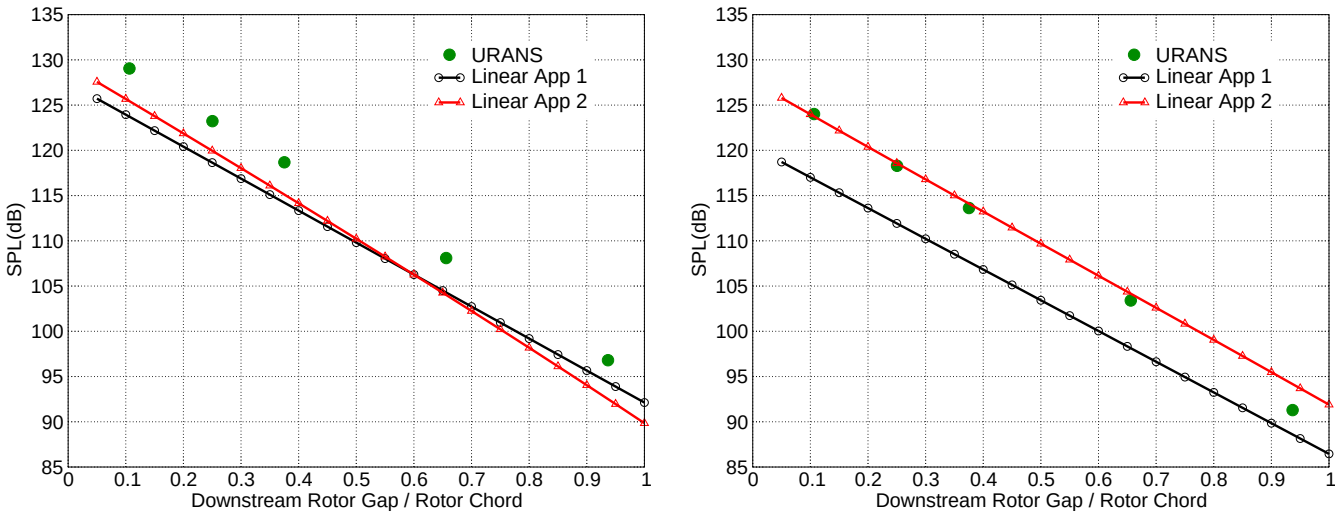

Figure 6: Inviscid Fan with No Loading: Noise levels at the inlet (left) and at the outlet (right). Black line is used to represent approach 1, whereas the red line is used for the approach 2. The results obtained with the non-linear code for the five builds are represented with green circles.

- The initial amplitudes of the potential fields are also defined at the leading edge and the trailing edge of the rows. As mentioned, this amplitude behave as a linear perturbation in a uniform flow even when we are very close to the blade. This behavior is also seen in the phase, which has a linear variation with the axial distance similar to what observed on regards the amplitude.

The total inlet and outlet noise levels obtained with this linear methodology are shown in Figure 6. Two different approaches have been investigated that consist on the consideration (Approach 1, A1) / non-consideration (Approach 2, A2) of the transmission of mode 0 through the rows. Thus A1 takes into account that the noise levels at inlet and outlet are only generated by the potential fields of both rows, neglecting the transmission process. In this situation, the iterative process explained in section 3 would finish at iteration 1, whereas in A2 the amplitudes obtained at iteration 1 at the middle-gap upstream and downstream propagating are transmitted through the rows in the following iterations. It is very interesting to see that the consideration of the transmission of mode 0 improves the results obtained with A1. This is specially remarkable at the outlet, where the noise levels obtained with A1 are under-predicted 8 dB. The noise levels at the inlet are also improved with the consideration of the transmission process of Mode 0. In fact, the slope of the noise level dependence with the gap/chord is more similar to that in the non-linear simulation. From Figure 6-left is also remarkable the difference in the noise-level between the linear method and the non-linear simulations. A discrepancy of 3 dB could be related to the absence in the linear model of other generation mechanisms of Mode 0. Another explanation can be found in non-linear mechanisms being responsible of the discrepancy. However, it is thought that the discrepancy is mainly due to uncertainties in the calculation of the reflection and transmission coefficients in the linear calculations. They are expected to be higher in the upstream propagating waves, consequently inlet noise, given that their phases changes more rapidly and are more sensitive to uncertainty errors. To finish with, Figure 7 shows, for Build 3, the results of the iterative process calculated with LMSOL for the interaction Mode 0 at inlet (upstream), middle gap (up and downstream) and outlet gap (downstream). It can be seen that 2 virtual iterations are sufficient since the amplitudes generated beyond are 30 dB lower. However, it is also seen that the use of only the first iteration, as done in some analysis [4, 12], can conduce to significant errors.

V. Application to a Viscous LP Turbine Interaction

The second case investigated is a 2D rotor-stator configuration corresponding to typical LP Turbine profiles. This can be seen as one step further than the inviscid test case, with a more complicated geometry where non-linear

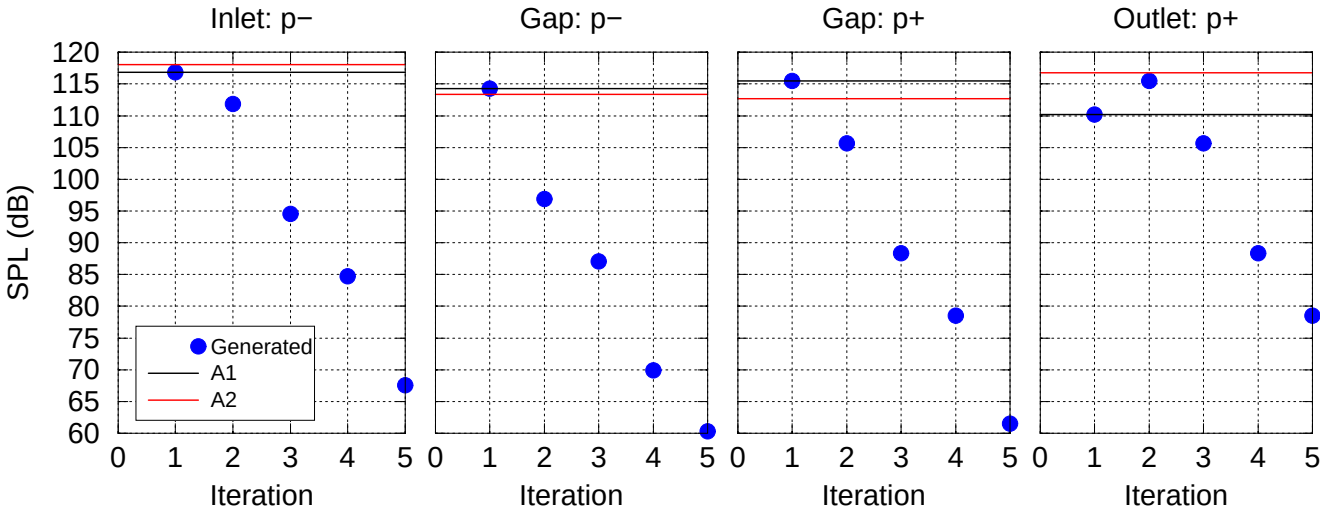

Figure 7: Inviscid Fan with No Loading Build 3: Reconstructed and virtual iterations amplitude for interaction Mode 0 at inlet (upstream propagating), middle (up and downstream propagating) and outlet (downstream propagating).

BUILD	Gap/chord
3	0.1007
4	0.1998
5	0.3998
6	1.0065
10	0.7207
11	0.6000
12	0.8000

Table 2: Non-linear simulations performed for the LP turbine case: each build correspond to a different value of the gap distance between the rows

effects could play a more important role, also with the inclusion of the viscosity leading unsteady generation sources of the same order as the main or viscous flow.

Similar to what was presented for the inviscid fan, the objective is to investigate the noise interaction sources for different distances between the rows, firstly with the URANS mode, secondly using LRANS, and to conclude consequently when the non-linear effects become important, if any. URANS simulations have been done for seven gap distances going between 10 and 100% (Table 2) and at a certain take-off representative condition. A fully turbulent Baldwin-Lomas [3] model has been used to model turbulence. Only one pitch is run without phase-lagged conditions given that the number-off selected for both rows is 94. The grid used is unstructured in the inviscid region, with a tangential number of modes able to solve second harmonics. A structured grid near the blade is used with boundary layer resolution based on dimensionless wall distance, y^+, less than unity. The number of points over the vane is sufficiently high to properly resolve the aerodynamics. Figure 8 shows different views of the computational domain and grid for Build 10. The total number of nodes goes from 170000 to 190000 depending on the gap distance. Inlet gap is set to one rotor axial chord, being two stator axial chords for the outlet. This is done to properly estimate the acoustics, as well as to avoid reflections as 1D Unsteady Non-Reflecting Boundary Conditions (UNRBC) have been imposed at the rotor inlet and stator outlet.

V.A Analysis on the Base or Main Flow.

Figure 9 shows the instantaneous Mach Number contours extracted from the URANS calculation, and for the shortest (left) and longest (right) distance between rows. From the comparison of these two figures, it can clearly

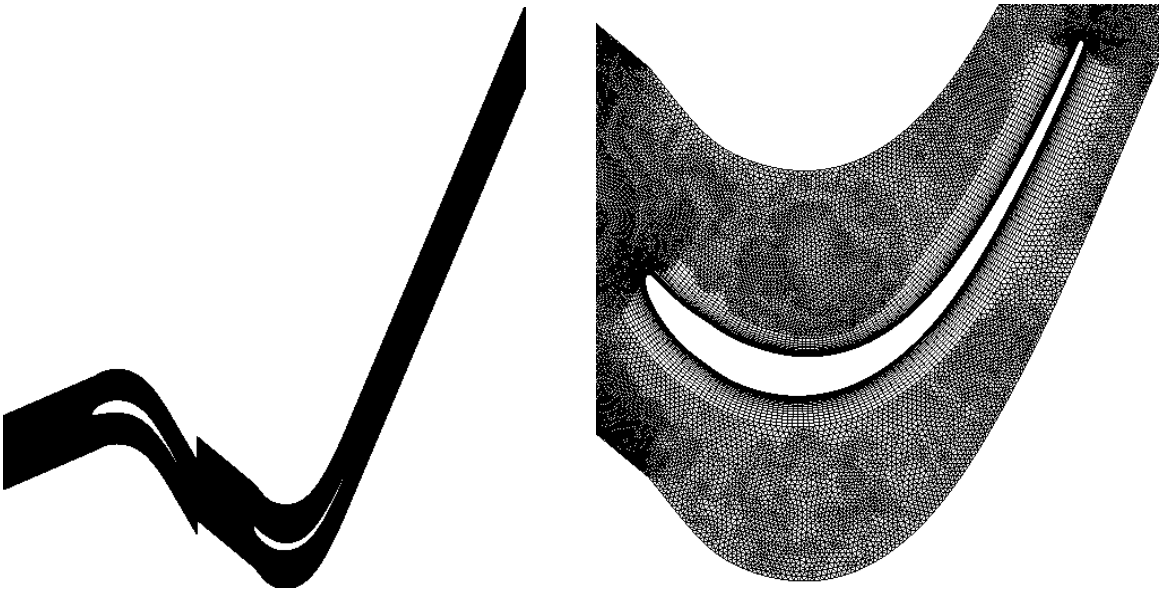

Figure 8: LP Turbine Interaction Build 10: Computational domain/grid (left) and vane profile grid detail (right).

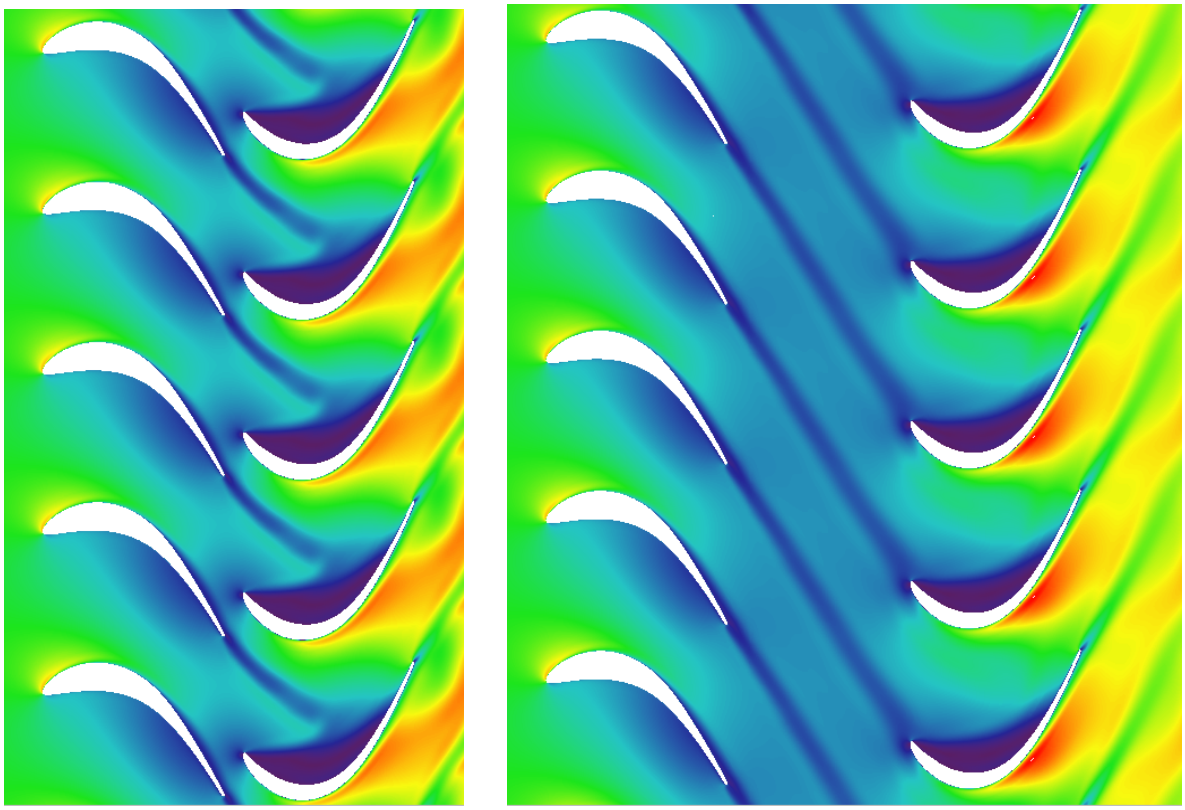

Figure 9: LP Turbine Interaction Builds 3 (left) and 6 (right). URANS results. Instantaneous Mach Number contours.

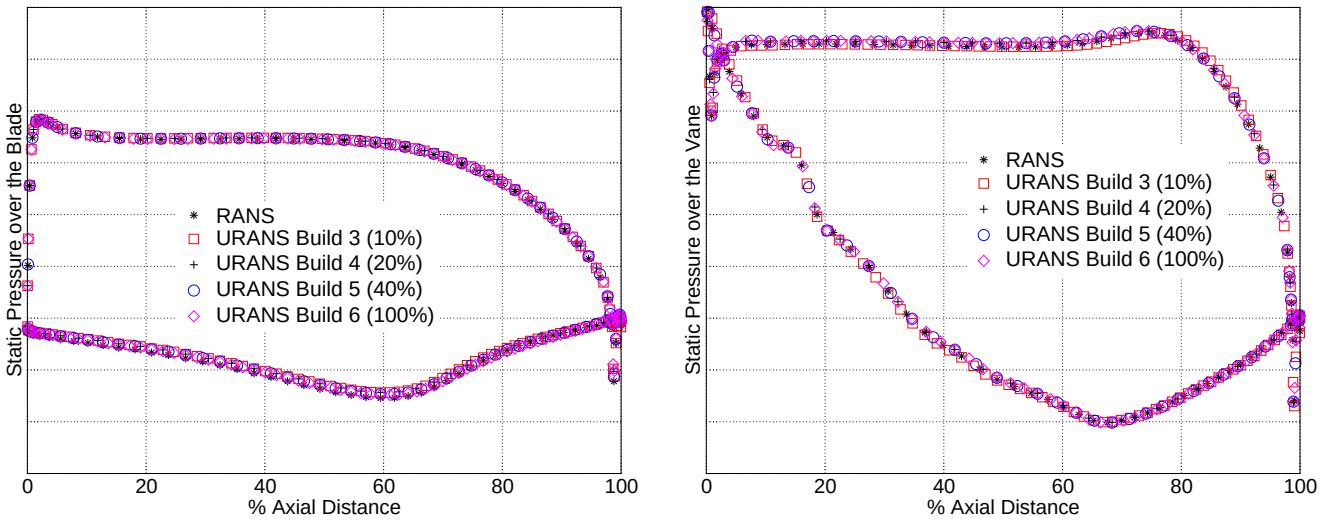

Figure 10: LP Turbine Interaction: Main Flow comparison for RANS and URANS time averaged solution for different distances between rows. Static pressure over the blade (left) and vane (right).

be seen that the presence of the adjacent rows change significantly the instantaneous aerodynamics of each row when the gap is small.

The influence of unsteadiness on the base or main flow can be observed by the comparison of time averaged URANS solutions to those that are obtained from independent single row RANS calculations using the same grid criteria, flow model, and averaged boundary conditions. The results are shown in Figure 10, particularly, the static pressure distribution over the blade (left) and vane (right) and from the RANS and several URANS time averaged solutions for different distances between rows. In can clearly be seen the high similarity between all the solutions, in other words, the presence of the adjacent row does not affect significantly the aerodynamics around the vane. It is important to remark that the boundary layer of the profiles is assumed to be fully turbulent from the leading edge, therefore no suction side bubble is present. These two effects, i.e., turbulent transition and suction side bubble, that are present in modern LP turbine designs could lead to discrepancies when comparing RANS vs URANS time averaged solutions, and a more detailed analysis for investigating these effects are out of the scope of this work.

Although aerodynamics near the profile has been found to be similar, it is interesting to note significant discrepancies in the wake mixing region, as shown in Figure 11, in which the pitchwise Stagnation Pressure distribution at 40% (left) and 100% (right) gap to vane chord downstream the stator is compared for the same builds as in Figure 10. Discrepancies appear not only between RANS and URANS models, but also depending on the distance between rows and also the distance between the wake profile and the vane: at 40% wake mixing of the shortest gap (Build 3) is similar to the RANS solution whereas at 100% vane chord downstream is more similar to the other URANS solutions.

In summary, those profiles with no suction side bubble or transient boundary layers, the presence of adjacent rows primarily affects the wake mixing mechanism, so that the distance between rows and downstream the vane are important. These findings are in line with those from Adamczyk [1, 2], so that performance dependencies (and consequently noise) with distance between rows in multi-stage turbines and compressors are primarily attributed to the wake mixing losses changes that are due to the non-linearity of the process with the time.

V.B Analysis on the Unsteady Flow.

Similar to the Inviscid Fan in Section 4, Figure 12-left shows, for the 70% Gap URANS solution, the amplitude of the relevant spinning modes in the inlet, outlet and middle gaps, i.e., Mode 94, -94 and interaction Mode 0. Figure 12-right shows, in dB scale, the amplitude of the vorticity waves for the same spinning modes. As expected, there are not significant vorticity amplitudes associated to the interaction Mode 0, whereas Mode -94 vorticity is only significant downstream the stator in which the aerodynamic losses at this frequency and mode has been

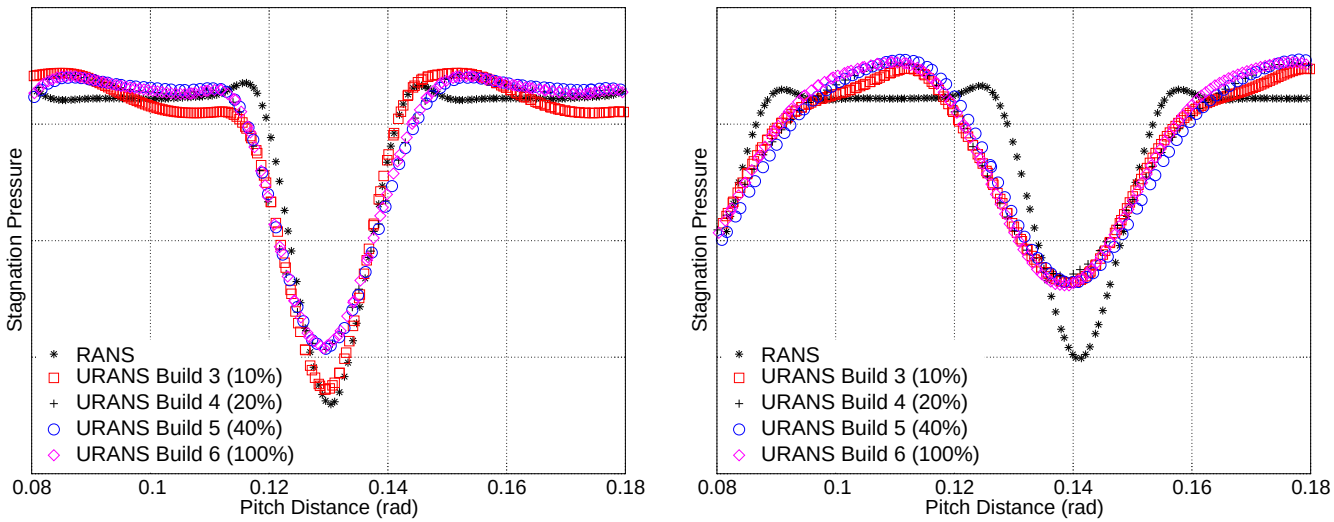

Figure 11: LP Turbine Interaction: Main Flow comparison for RANS and URANS time averaged solution for different distances between rows. Pitchwise Stagnation Pressure distribution for 40% (left) and 100% (right) gap to vane chord downstream the stator.

generated. Differently to the inviscid fan, interaction noise in this case will be due to potential and mainly wake noise, something that cannot be demonstrated with the URANS results but with the use of independent LRANS calculations.

Figure 13 shows the split of the URANS solution shown in Figure 12 into up and downstream acoustic sources (left and right plots respectively). These results, together with the vorticity plot shown in Figure 12-right, are not directly obtained from the URANS and they correspond to a wave splitting technique to separate unsteady disturbances that is detailed in the Appendix. This technique assumes that the main flow is uniform, something that does not happen in this case, so that circumferentially averaged flow magnitudes have been used for the decomposition in waves. A consequence of the non-uniformities of the flow is that the waves obtained do not behave as ideally expected, i.e., cut-on acoustic waves and vorticity with constant amplitude or cut-off waves decaying exponentially. This will be another subject of uncertainties when evaluating URANS solutions from independent LRANS calculations, as it will be explained in this section.

As mentioned, given that the simulations are viscous, the mechanisms responsible of the generation of the interaction Mode 0 are not only the potential field coming from rotor and stator, but also the viscous wake from the rotor that impinges the stator. The number of modes and perturbations considered will be therefore based on these three main mechanisms. They are Mode 94, Mode -94 and the interaction Mode 0. Although this is the same number of modes that were used in the inviscid fan, in this case five linear simulations are necessary due to the presence of the rotor wake:

- Rotor wake impinging the stator (mode 94, v)
- Potential field of stator upstream propagating and interacting with the rotor (mode -94,-)
- Potential field of rotor downstream propagating and interacting with the stator (mode 94,+)
- Transmission through the rotor of interaction mode propagating upstream (mode 0,-)
- Transmission through the stator of interaction mode propagating downstream (mode 0,+)

The transmission and reflection coefficients are calculated in the same way explained in Section 4. As mentioned, in this case the flow is highly non-uniform and the acoustic and vorticity modes do not behave as in a uniform flow, introducing further uncertainties on the estimation of the coefficients. To illustrate this, Figure 14 shows the evolution of the acoustic Mode 0 generated in the interaction between the rotor wake and the stator. The following considerations are taken from that figure:

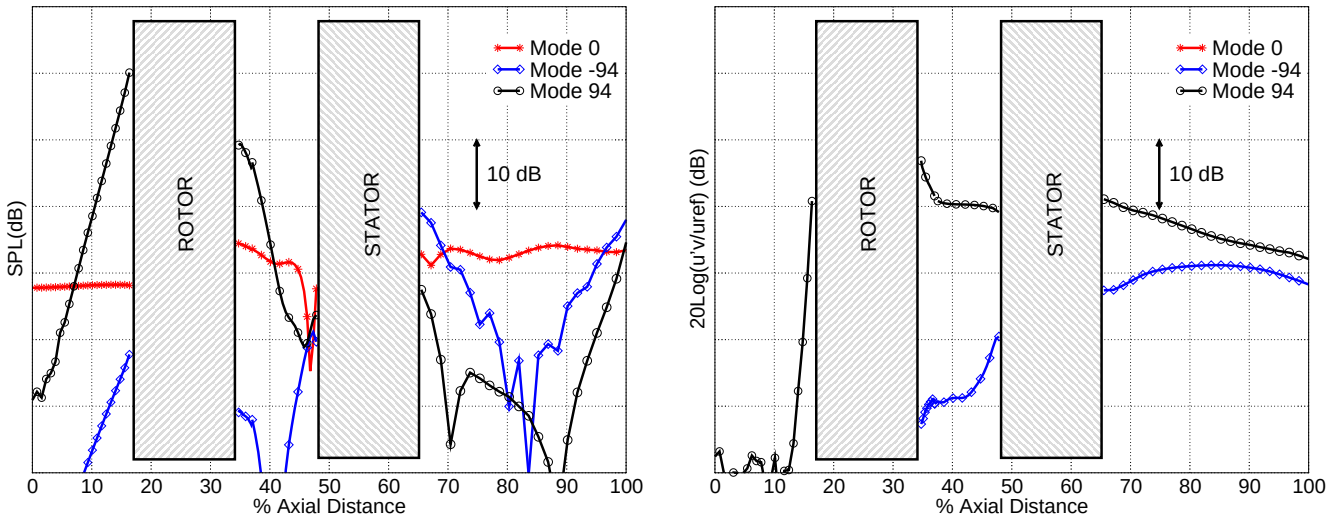

Figure 12: LP Turbine Interaction Build 10 URANS solution: Spinning mode amplitudes of the relevant modes contributing to the 1BPF (left) and amplitudes of the vorticity intensities (right).

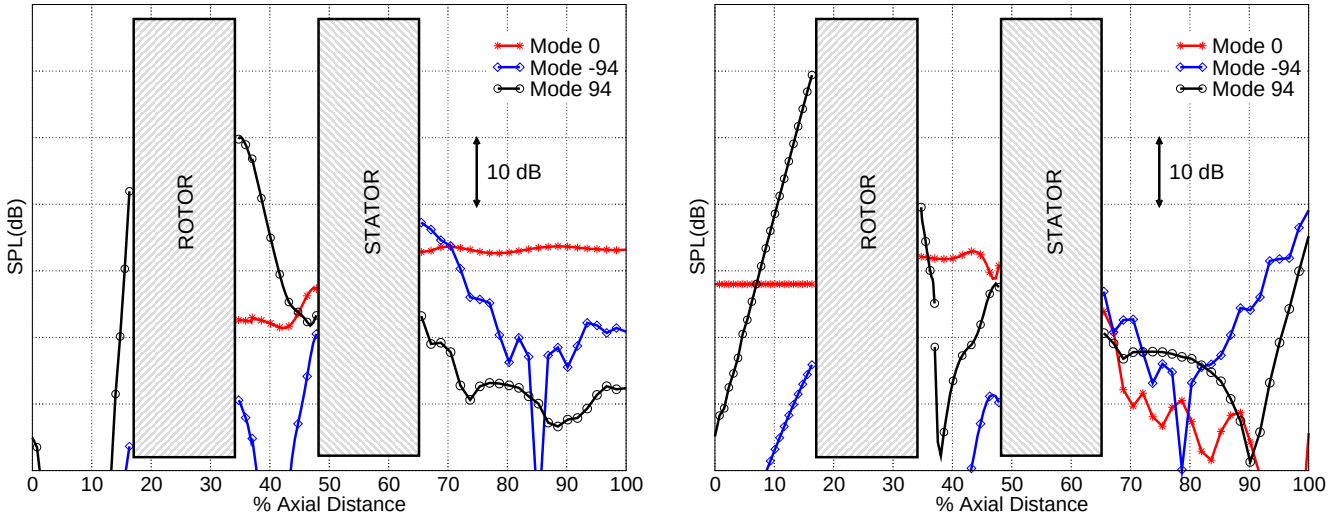

Figure 13: LP Turbine Interaction Build 10 URANS solution: Spinning mode amplitudes of the relevant modes contributing to the 1BPF. Downstream Propagating / Decaying waves (left). Upstream Propagating / Decaying waves (right).

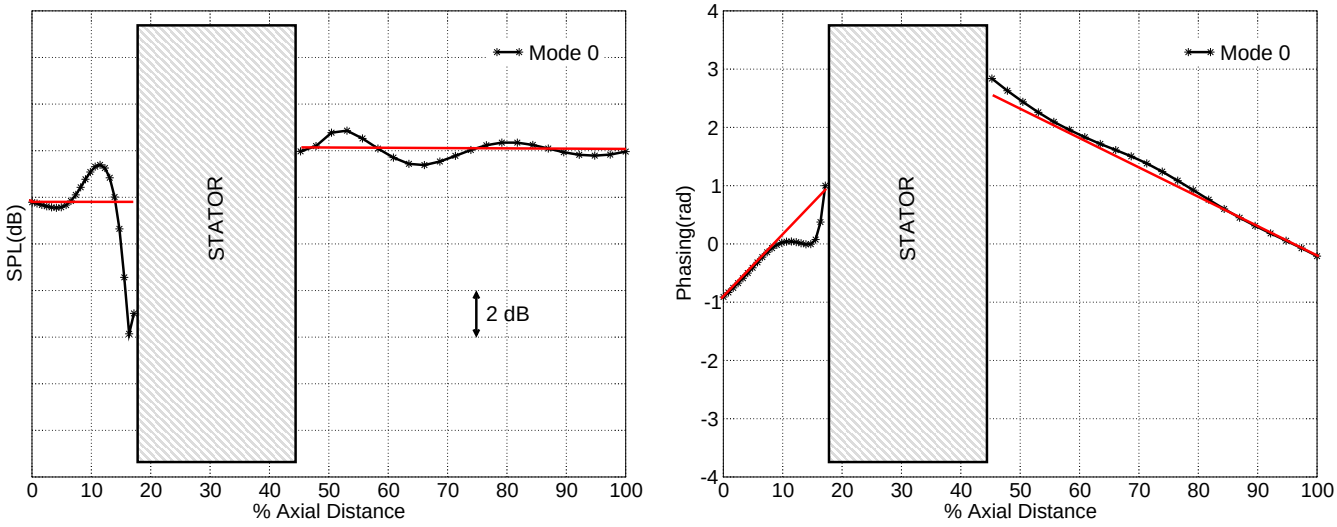

Figure 14: Linear simulation of rotor wake in stator row. The amplitude (left) and phase (right) of the mode 0 propagating upstream is represented with a red line, whereas the downstream propagation at the outlet is represented with a black line.

- The cut-on mode needs a distance to be generated. The single-row used for the linear simulations must have gaps long enough to allow the generation of the modes [11].
- As stated before, the amplitude of the mode is not constant due to a non-uniform steady flow. The oscillations depend on the the non-uniformities that the steady flow has: whereas the oscillations in the upstream propagating mode rapidly disappear as they are due to the potential field that decays exponentially, the oscillations downstream do not disappear as they are due to the presence of the steady wake. This fact has important consequences in the definition of the reflection and transmission coefficients, as average amplitudes represented by the red lines ar taken, as shown in Figure 14-left.
- The behavior of the phase is not as affected as the amplitude. However, the behavior of the phase is not linear near the blade and a linear behavior has been supposed represented by the red lines shown in Figure 14-right.

The initial perturbations vector is formed of the three generation mechanisms mentioned above: stator potential field, rotor potential field and rotor wake. It is important to remark that the evolution of the rotor wake in the middle-gap is not completely captured with the linear code. Whereas it is able to predict the change in its phase, the viscous mixing of the wake is a non-linear phenomenon that cannot be estimated. However, this effect is only important for very low gaps where the amplitude changes rapidly. The criteria followed to fix the initial amplitude of the wake is the use of the amplitude that reaches the stator leading edge at each build.

Three approaches have been considered in the estimation of the non-linear noise levels via linear calculations. They serve to conclude with regard the relative weight of the generation mechanisms as well as with the importance of the transmission process:

- Approach 1 (A1): mode 0 is generated only due to the interaction between the rotor wake and the stator. Potential fields and transmission are neglected.
- Approach 2 (A2): together with the wake interaction, the transmission of mode 0 is considered (A1 + transmission). Potential fields are neglected.
- Approach 3 (A3): wake, potential field and transmission are included (A2 + potential fields).

Figure 15 shows the noise levels obtained at the inlet (left) and outlet (right) of the domain. Paying first the attention on the left plot, the following can be concluded:

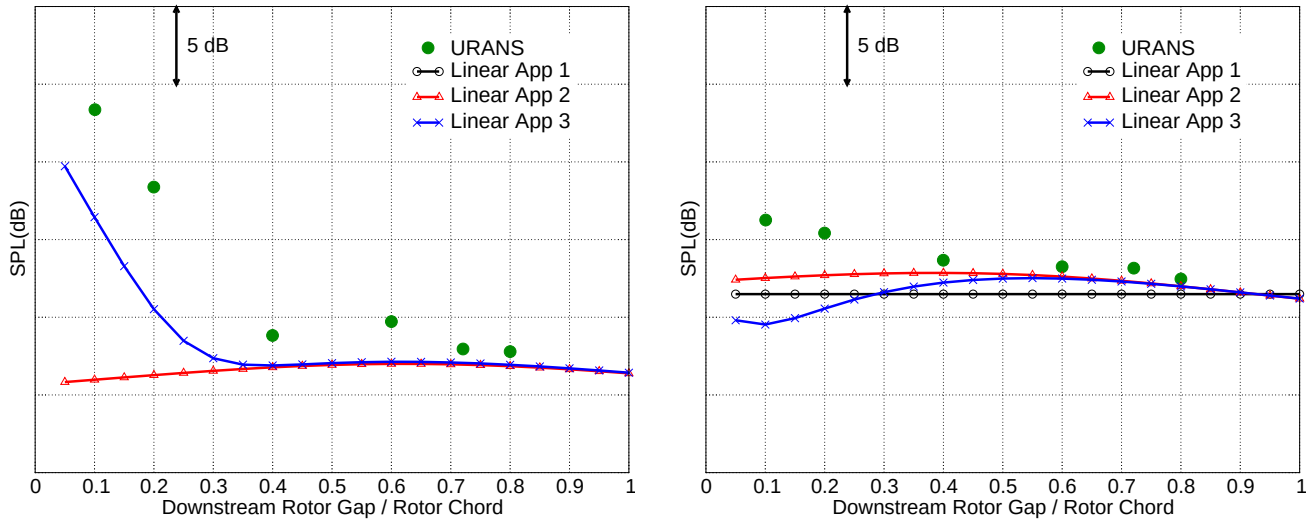

Figure 15: Noise levels at the inlet (left) and at the outlet (right). Black line is used to represent approach 1. Red line is used for the approach 2, whereas the blue line represents approach 3. The results obtained with the non-linear code for the seven builds are represented with green circles.

1. The rotor wake and the transmission of Mode 0 are the dominant mechanisms in the noise generation at the inlet for gap to chord values greater than 0.4. It is important to remark that the inclusion of the transmission process is necessary to have noise at the inlet; in other case no noise can be generated with the only presence of the rotor wake.

2. For this range of gap/chord > 0.4, an under-prediction of 3 dB exists at the inlet, similar to what was obtained for the inviscid fan.

3. For gap/chord lower than 0.4, the potential field becomes an important source of noise with interaction noise levels comparable to the wake interaction ones.

4. Even with the inclusion of the potential field, the under-predictions are up to 8 dB at the inlet for that range of gap/chord < 0.4 . This discrepancy is greater than that observed for the inviscid fan, which was attributed to methodology uncertainties. In this case the reason is found in the great amplitude of the perturbation, which does not allow the linearization as it is not valid the uncoupling of the steady and the unsteady field.

The conclusions for the results at the outlet go in the same direction as those of the inlet:

1. Rotor wake interacting with the stator is the dominant mechanism in the generation of the noise level at the outlet for gap to chord values greater than 0.4. A better agreement with a maximum under-estimation of 1dB is obtained with the inclusion of the transmission process, although its importance is of second order. The potential field has no incidence on the noise levels at the outlet.

2. For gap/chords < 0.4, an under-prediction of the noise level of up to 5 dB exists. The inclusion of the potential field is not able to explain that discrepancy; the reason is thought to be again the non-linear effects associated to the wake.

Figure 16 shows the iterative process for Build 5 (40% gap to rotor chord) in which a number of 5 virtual iterations are sufficient. Whereas inlet noise is highly dependent on transmission and reflection events so that iteration 2 is also significant, outlet noise is broadly dominated by the noise emitted from the wake, being the rest of virtual iterations more than 10 dB lower.

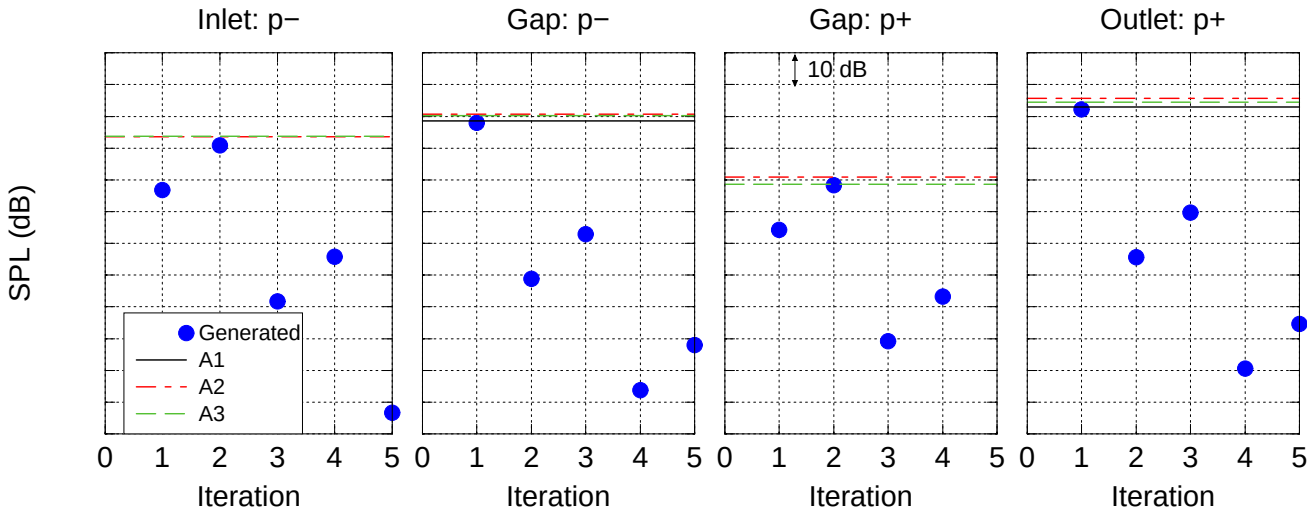

Figure 16: LP Turbine Interaction Build 5 URANS solution: Reconstructed and virtual iterations amplitude for interaction Mode 0 at inlet(upstream propagating), middle(up and downstream propagating) and outlet(downstream propagating).

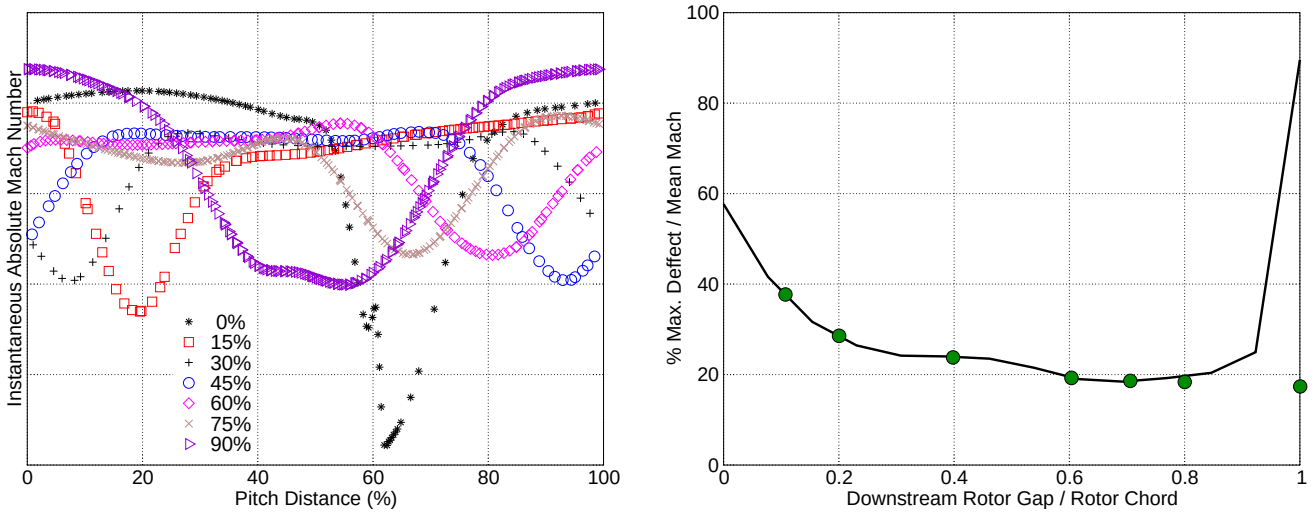

Figure 17: LP Turbine Interaction Build 6 URANS solution (100% gap to rotor chord): Instantaneous Mach Number profiles at selected gap to rotor chord distances (left). Maximum depth to Mean Mach Number ratio as a function of distance (right). The simulation chosen has a gap that is not long enough to have an undisturbed wake at every cut, being those done at a distance between 0.8 and 1 chord disturbed by the stator potential field (black line). Wake intensities corresponding to g/c of 0.8 and 1 are guessed from the tendency (green circles).

As mentioned, the non-linearities associated to the wake for low gap/chords can produce an excess of noise. Figure 17-left shows the instantaneous Mach Number distribution for Build 6 (100% gap to rotor chord distance) and different axial positions between the two rows. The velocity defect (wake depth), defined as the maximum Mach Number depth related to the mean value, is plotted in 17-right for the same simulation, together with the corresponding gap to chord ratio of the different URANS builds. Combining the results from Figures 15 and 17, it is concluded that the largest under-predictions in the noise levels could be related with the highest intensities of the wakes that impinge the stator. Non-linear effects (interaction between harmonics) due to wake depths higher than 20% could be responsible of high non-linear noise levels. It is interesting to remark that the simulation chosen to obtain the Figure 17-right has a gap that is not long enough to have an undisturbed wake at every cut, being those done at a distance between 0.8 and 1 chord disturbed by the stator potential field (black line), so that wake intensities corresponding to Builds 12 (80%) and 6 (100%) are guessed from the situation in which the stator were not present (green circles).

VI. Conclusions

The linearity of Turbomachinery Interaction Noise have been investigated by the comparison of URANS and LRANS fluid models. Unsteady term responsible of possible non-linearities has been identified based on the incompressible convective term, result that can be easily extended to the full RANS equations. A methodology for predicting interaction noise based on independent single row LRANS calculations have been presented, firstly for one mode, 2D flow and two rows, and then extended to a general case.

The methodology is verified with a first set of URANS versus LRANS comparisons based on an inviscid fan 2D geometry with no loading and different distances between the rows. The potential field is sufficiently low so that the interaction can be considered linear. URANS and LRANS give similar results at the outlet domain and discrepancies in inlet noise are about 3 dB, something that is attributed to uncertainties in the calculation of the linear coefficients, since upstream propagating waves are more sensitive as the phasing changes more rapidly.

A second set of viscous 2D simulations, with LP Turbine rotor and stator geometries and different distances between the rows have been used for assessing the linearity of interaction noise. The comparison of the single row RANS calculation and time averaged URANS solutions shows that the presence of an adjacent row in relative motion does not affect the time averaged static pressure over the airfoil; however it changes significantly the wake mixing mechanisms. Reconstruction of interaction noise based on independent LRANS calculations shows that noise is dominated by wake interaction when the gap to chord ratio is sufficiently high. For lower than 40% values, the presence of the potential noise starts to be relevant as well as the discrepancies between URANS and LRANS models are significant, indicating that the non-linear source of noise starts to be dominant.

The extension of this study to 3D geometries, including LP Turbine modern design styles, will be subject of a second part of this paper to be published in 2012.

Acknowledgments

This analysis has been funded by ITP.

Appendix: Wave Splitting in 2D Uniform Flows

Assuming the unsteady flow as small perturbations of the main or steady flow, that is uniform and 2D, and that unsteady perturbations are harmonic as:

$$\begin{bmatrix} \rho^d \\ u^d \\ v^d \\ p^d \end{bmatrix} = \mathfrak{Re}\left\{ \begin{bmatrix} \rho' \\ u' \\ v' \\ p' \end{bmatrix} e^{i(\omega t + k_y y + k_x x)} \right\} \tag{9}$$

The Linearized Euler Equations are:

$$\frac{\rho'}{\rho_0}(\omega + u_0 k_x + v_0 k_y) + k_x u' + k_y v' = 0 \tag{10}$$

$$u'(\omega + u_0 k_x + v_0 k_y) + \frac{k_x}{\rho_0} p' = 0 \tag{11}$$

$$v'(\omega + u_0 k_x + v_0 k_y) + \frac{k_y}{\rho_0} p' = 0 \tag{12}$$

$$k_x u' + k_y v' + \frac{p'}{\gamma \cdot p_0}(\omega + u_0 k_x + v_0 k_y) = 0 \tag{13}$$

They can be expressed in a dot-matrix form:

$$\begin{bmatrix} (\omega + u_0 k_x + v_0 k_y) & k_x \rho_0 & k_y \rho_0 & 0 \\ 0 & (\omega + u_0 k_x + v_0 k_y) & 0 & k_x \\ 0 & 0 & (\omega + u_0 k_x + v_0 k_y) & k_y \\ 0 & \gamma p_0 k_x & \gamma p_0 k_y & (\omega + u_0 k_x + v_0 k_y) \end{bmatrix} \begin{bmatrix} \rho' \\ u' \\ v' \\ p' \end{bmatrix} = \begin{bmatrix} 0 \\ 0 \\ 0 \\ 0 \end{bmatrix} \tag{14}$$

Non-trivial solutions will be those satisfying:

$$(\omega + u_0 k_x + v_0 k_y)^2 \left[\rho_0 (\omega + u_0 k_x + v_0 k_y)^2 - \gamma p_0 \left(k_x^2 + k_y^2\right)\right] = 0 \tag{15}$$

Obtaining a double root solution associated to entropy and vorticity disturbances and another two roots associated to up and downstream acoustic propagating waves. In summary:

Eigenvalue	Eigenvector
$k_x = -\frac{k' + M_y k_y}{M_x}$	$\begin{bmatrix} \rho' \\ u' \\ v' \\ p' \end{bmatrix} = \begin{bmatrix} 1 \\ 0 \\ 0 \\ 0 \end{bmatrix}$
$k_x = -\frac{k' + M_y k_y}{M_x}$	$\begin{bmatrix} \rho' \\ u' \\ v' \\ p' \end{bmatrix} = \begin{bmatrix} 0 \\ 1 \\ -\frac{k_x}{k_y} \\ 0 \end{bmatrix}$
$k_x^+ = \frac{M_x(k + k_y M_y) - \sqrt{(k + k_y M_y)^2 - k_y^2(1 - M_x^2)}}{1 - M_x^2}$	$\begin{bmatrix} \rho' \\ u' \\ v' \\ p' \end{bmatrix} = \begin{bmatrix} \frac{1}{c_0^2} \\ -\frac{k_x^+}{\omega + u_0 k_x^+ + v_0 k_y} \\ -\frac{k_y}{\omega + u_0 k_x^+ + v_0 k_y} \\ 1 \end{bmatrix}$
$k_x^- = \frac{M_x(k' + k_y M_y) + \sqrt{(k' + k_y M_y)^2 - k_y^2(1 - M_x^2)}}{1 - M_x^2}$	$\begin{bmatrix} \rho' \\ u' \\ v' \\ p' \end{bmatrix} = \begin{bmatrix} \frac{1}{c_0^2} \\ -\frac{k_x^-}{\omega + u_0 k_x^- + v_0 k_y} \\ -\frac{k_y}{\omega + u_0 k_x^- + v_0 k_y} \\ 1 \end{bmatrix}$

Under these circumstances, it can be concluded that the Eigenvalue problem is a Sturm-Liouville one so that any perturbation admits an unique decomposition into vorticity, entropy and up / down acoustic propagating waves.

References

[1] Adamcyzk, J.J., *Aerodynamic Analysis of Multistage Turbomachinery Flows in Support of Aerodynamic Design*. ASME Journal of Turbomachinery, vol. 122, pp. 189-217, 2000.

[2] Adamcyzk, J.J., *Model Equation for Simulating Flows in Multistage Turbomachines*. ASME paper 85-GT-226.

[3] Baldwin, B. S., Lomax, H. *Thin Layer Approximation and Algebraic Model for Separated Flows*. AIAA Paper, 78-257, 1978.
[4] Broszat, D., Korte, D., *Validation of Turbine Noise Prediction Tools with Acoustic Rig Measurements*. AIAA paper, 2009-3283.
[5] Burgos, M.A., Contreras, J. and Corral, R., *Efficient Edge-Based Rotor/Stator Interaction Method*. AIAA Journal, Vol. 49, No. 1, pp 19-31, January 2011.
[6] Burgos, M.A., Contreras, J., Corral, R., *Numerical Treatment of the Rotor/Stator Interaction Problem in Unstructured Grids*. AIAA paper, 2007-4474.
[7] Corral, R., Crespo, J., and Gisbert, F. *Parallel Multigrid Unstructured Method for the Solution of the Navier-Stokes Equations*. AIAA Paper 2004-0761, 42nd AIAA Aerospace Sciences Meeting and Exhibit, Reno, January 2004.
[8] Corral, R., Escribano, A., Gisbert, F., Serrano, A., and Vasco, C. *Validation of a Linear Multigrid Accelerated Unstructured Navier-Stokes Solver for the Computation of Turbine Blades on Hybrid Grids*. AIAA Paper 2003-3326, May 2003.
[9] Envia, E., Tweedt, D., Woodward, R.P., Elliot, D.M., Fite, E.B., Hughes, C.E., Podboy G.G., Sutli, D.L., *An Assessment of Current Fan Noise Prediction Capability*. AIAA paper, 2008-2991, 2008.
[10] Escribano, A.G., Serrano, A., Corral, R., Vasco C., *LP Turbine Interaction Noise Generation and Transmission Analysis based on 2D Linear CFD Calculations*. AIAA paper, 2003-3137.
[11] Escribano, A. G., Serrano, A. and de la Calzada, P., *Investigation on Numerical and Geometry Modelling Effects on the CFD Simulation of Interaction Noise in LP Turbines*. 5th European Conference on Turbomachinery Fluid Dynamics and Thermodynamics. Prague, Czech Republic. March 2002.
[12] Kennepohl F., Kahl G., Heinig K.. *Turbine Blade/Vane Interaction Noise: Calculation with a 3D Time-Linearised Euler Method*. AIAA paper, 2001-2152. May 2001.
[13] Giles, M.B., *Non-reflecting Boundary Conditions for Euler Equation Calculations.* AIAA Journal, Vol. 28, No. 12, pp. 2050-2057, 1990.
[14] Heinig, K.E. *Sound Propagation in Multistage Axial Flow Turbomachines*. AIAA Journal, Vol 21., No. 1, pp 98-105, 1982.
[15] Maunus, J., Grace, S.M., Sondak, D.L., *Effect of Rotor Wake Structure on Fan Interaction Noise*. AIAA paper, 2010-3746.
[16] Nesbitt, E., *Towards a Quieter Low Pressure Turbine: Design Characteristics and Prediction Needs*. International Journal of Aeroacoustics, Vol 10., Number 1, pp 1-15, August 2010.
[17] Pinelli, L., Poli, F., Marconcini, M., Arnone, A., Spano, E., Torzo, E., *A Linearized Method for Tone Noise Generation and Propagation in a Multistage Contra-Rotating Turbine*. 9th European, Conference on Turbomachinery Fluid Dynamics and Thermodynamics, Istanbul, Turkey, March 2011.
[18] Serrano, A., *Linearized CFD Techniques Applied to Low Noise Designs in Turbines*. Proceedings of the AARC Workshop in Turbine Noise, Vancouver, BC, May 2008.
[19] Serrano, A., Fernández Aparicio, J.R., Vázquez, R., *On the estimation and relevance of internally generated turbine broadband noise.* International Journal of Aeroacoustics, volume 10, number 1, August 2010, pp 51-74.
[20] Sharma, A., Chen, H., Shieh, C.M., *Linearized Navier-Stokes Analysis for Rotor-Stator Interaction Tone Noise Prediction.* AIAA paper, 2010-3744.
[21] Sijtsma, P., Rademaker, E.R. and Schulten, J.M.H.M., *Experimental Validation of Lifting Surface Theory for Rotor-Stator Interaction Noise Generation.* AIAA Journal, Vol. 36, No. 6, pp. 900-906, June 1998.
[22] Schulten, J.B.H.M., *Sound Generation by Ducted Fans and Propellers as a Lifting Surface Problem*. PhD Thesis, Twente University, July 1941.
[23] Tyler, J.M. , Sofrin, T.G., *Axial Flow Compressor Noise Studies*. SAE Transactions, Vol 70, pp 309-332, 1962.
[24] Van Zante, D., *Large-Scale Simulations for Turbine Engine Core Noise.* International Journal of Aeroacoustics, Vol 10, Number 1, August 2010.
[25] Weir, D.S., Mendoza, J.M., *Baseline Noise Measurements from the Engine Validation of Noise and Emissions Reduction Technology Program*. AIAA paper, 2008-2807, 2008.